JACS
JOURNAL OF THE AMERICAN CHEMICAL SOCIETY
Article
pubs.acs.org/JACS

Chain-Reaction Anion Exchange between Metal–Organic Cages

Shucong Ma, Maarten M. J. Smulders,† Yana R. Hristova, Jack K. Clegg,‡ Tanya K. Ronson, Salvatore Zarra, and Jonathan R. Nitschke*

Department of Chemistry, The University of Cambridge, Lensfield Road, Cambridge CB2 1EW, United Kingdom

Supporting Information

ABSTRACT: Differential binding affinities for a set of anions were observed between larger (**1**) and smaller (**2**) tetrahedral metal–organic capsules in solution. A chemical network could thus be designed wherein the addition of hexafluorophosphate could cause perchlorate to shift from capsule **2** to capsule **1** and triflimide to be ejected from capsule **1** into solution.

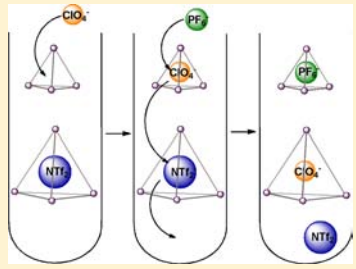

INTRODUCTION

In recent years, metal–organic capsules have attracted continued attention due to their wide-ranging applications as photoreactors,[1,2] in the stabilization of reactive species,[3,4] and in molecular recognition.[5−7] These abiological structures are also of relevance as functional mimics of biological molecules such as protein receptors[8−10] and enzymes.[11,12]

In a similar fashion to enzymes, container molecules can catalytically accelerate specific chemical transformations of their guests.[13−20] In a first step toward mimicking the elegant enzymatic "assembly lines" that construct the most complex and functional natural products,[21] systems of catalytic container molecules might be used to carry out sequences of reaction steps wherein the product of one capsule's transformation becomes the substrate for the next. The use of protective capsules in such sequences,[4,22−30] capable of storing and preventing other substrates' reactions, could allow more complex behavior within systems of transformative hosts.

As a precondition for designing systems of functional container molecules, it is necessary to explore and understand how multiple guests interact with different hosts in ways that allow for complex behavior to emerge.[31,32] In this study we explore a system of two metal–organic hosts[33−39] and multiple guests, in which differential binding affinities between hosts and guests allow transfer of a guest between hosts upon the addition of a competing guest, laying the groundwork for networks of capsules to accomplish sequential multistep transformations.

RESULTS AND DISCUSSION

The present system comprises metal–organic container molecule **1** (Scheme 1, top)[40] and previously reported **2** (Scheme 1, bottom),[41] both of which were prepared using subcomponent self-assembly,[42−44] and both of which were observed to bind anions with different affinities.

The reaction of 5,5′-(1,4-phenylene)bis-2-pyridinecarboxaldehyde (6 equiv), anisidine (12 equiv), and a suitable iron(II) salt (4 equiv) led to the formation of the dark-green $[Fe_4L_6]^{8+}$ cage complex **1** (Scheme 1, top). The C_2-symmetric bis-bidentate pyridylimine ligands form the edges of the tetrahedron, bridging between the four 6-coordinate iron(II) ions at the vertices. The cage exhibits simple ^{1}H and ^{13}C NMR spectra in solution (Figures S1 and S2), consistent with *T* point symmetry. Cage **1** was prepared from iron(II) tetrafluoroborate (**1**·$(BF_4)_8$), perchlorate (**1**·$(ClO_4)_8$), hexafluorophosphate (**1**·$(PF_6)_8$), or bis(trifluoromethane)sulfonimide (triflimide, **1**·$(NTf_2)_8$).

Other anilines could also be incorporated into the cage corners; anisidine was chosen for subsequent studies because the corresponding cage was easier to purify through recrystallization, enabling the isolation of crystals of sufficient quality for single-crystal X-ray diffraction analysis. It was determined that incorporation of different anilines does not affect the binding affinity of anions for cage **1** (Figure S30).

Single crystals of the triflimide salt of **1** of sufficient quality for X-ray analysis could not be obtained despite numerous attempts. However, crystal structures of both the tetrafluoroborate (Figure 1) and perchlorate salts of **1** (Figure S17) were obtained using synchrotron radiation at the Diamond Light Source.[45] The very small crystals were obtained by vapor diffusion of diisopropyl ether into acetonitrile solutions of the cage. Each Fe_4L_6 complex has approximate (although not crystallographic) *T* symmetry, with either a ΔΔΔΔ or ΛΛΛΛ configuration at the metal centers. The metal–metal separations are ∼13.4 Å, and the calculated cavity volume is approximately 245 Å^3, placing this cage among the larger M_4L_6 species synthesized.[40,46−48] The interior of **1** contains three acetonitrile molecules in the structure of **1**·$(BF_4)_8$, and a mixture of diisopropyl ether and acetonitrile in **1**·$(ClO_4)_8$.

Cage **1** was observed to bind the anions BF_4^-, PF_6^-, or NTf_2^-, as confirmed by ^{19}F NMR and a ^{1}H–^{19}F HOESY

Received: December 5, 2012
Published: March 18, 2013

dx.doi.org/10.1021/ja311882h | J. Am. Chem. Soc. 2013, 135, 5678−5684

Scheme 1. Formation of Cages 1 and 2 from Iron(II) and Either 5,5′-(1,4-Phenylene)bis-2-pyridinecarboxaldehyde and Anisidine (1) or 6,6′-Diformyl-3,3′-bipyridine and Aniline (2)

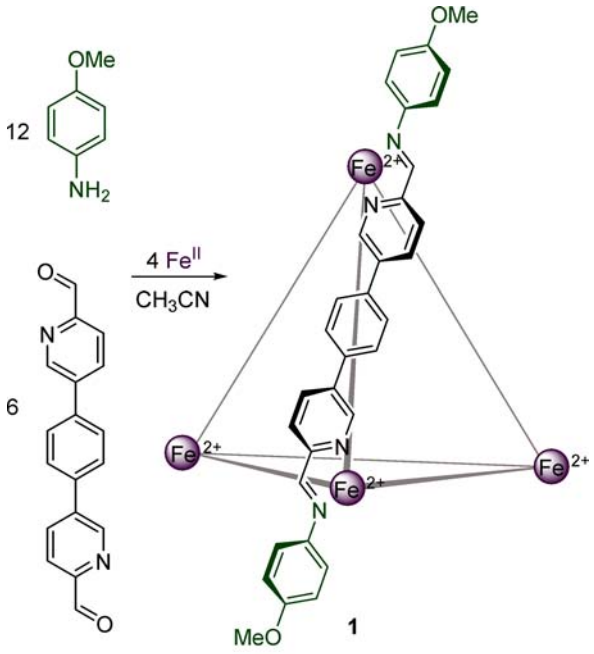

experiment (Figure S12) for cage $\mathbf{1}\cdot(PF_6)_8$, in which nuclear Overhauser correlations between PF_6^- resonances and peaks corresponding to the central phenylene and inward-facing pyridine protons of the ligand were observed. In each case, the ^{19}F NMR resonances for the guest molecules were broadened and shifted compared to the resonances of the anions in the absence of cage **1** suggesting fast exchange on the NMR time scale (Figures S3, S7, and S11).

In order to perform anion binding studies from an "empty" cage, we attempted to prepare cage **1** with a large counterion whose volume exceeds the cavity volume. However, when the synthesis of cage **1** was carried out with the larger counterions tetraphenylborate or tetrakis(3,5-bis(trifluoromethyl)phenyl)-borate, cage **1** was not observed to form, and only materials showing negligible solubility in common laboratory solvents were obtained.

An estimate of the binding constant of triflimide for **1** was obtained by titrating excess NTf_2^- (Figure S19) into an

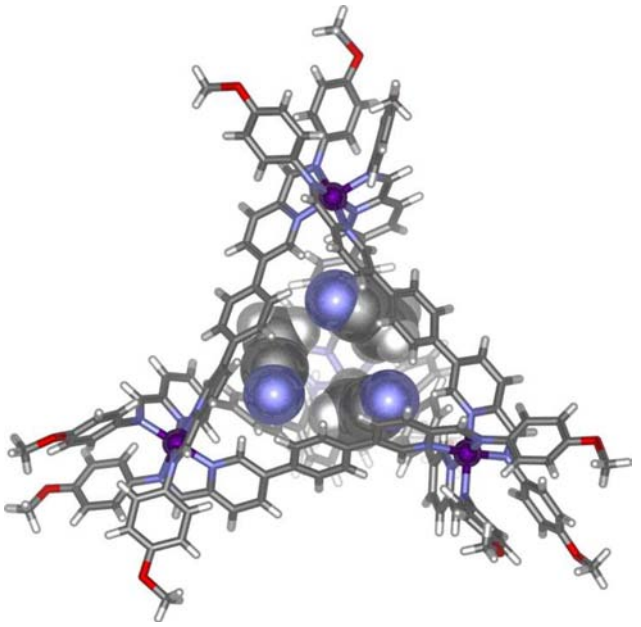

Figure 1. X-ray crystal structure of $[(MeCN)_3\subset\mathbf{1}]\cdot 8BF_4\cdot 0.5MeCN$. Anions and solvents outside of the central cavity are omitted for clarity. Only one location of the disordered encapsulated acetonitrile molecules is shown.

acetonitrile solution of $\mathbf{1}\cdot(NTf_2)_8$. Although it was not possible to obtain the entire binding isotherm due to the necessity of having to estimate the section between 0 and 8 equiv, the binding of NTf_2^- was moderate enough to allow observation of the isotherm above 8 equiv. The affinity of NTf_2^- was thus estimated to be $(1.4 \pm 0.5) \times 10^3\ M^{-1}$. The data fit well to a 1:1 binding model, and we infer the Coulombic and steric penalties incurred by forcing two triflimides into the same cavity to be prohibitive. We thus conclude that host **1** exhibits 1:1 binding with NTf_2^-.

In order to quantify the hierarchy of anion binding in host **1**, competitive titration experiments were performed. The titration of BF_4^-, OTf^-, PF_6^-, and ClO_4^- against cage $\mathbf{1}\cdot(NTf_2)_8$ in acetonitrile solution allowed the competitive binding constants of these four anions to be determined (Figures S23, S25, S27, and S29). Again 1:1 binding was found for all the anions, as concluded from the good fit of all titration curves to a 1:1 binding model. Cage **1** did not display strongly differential binding between these anions,[49−51] with the exception of perchlorate, which was observed to bind to cage **1** an order of magnitude more strongly than NTf_2^- (Table 1). The other anions bound 2−3 times more strongly than NTf_2^-; the quality of the data fitting allowed us to conclude that the differences between the best and worst of these binders are small but real.

Anion Exchange Studies. The different anion binding affinities of cage **1** allowed an anion displacement experiment to be carried out, which illustrated the exchange of bound anions within the system. When BF_4^- (8 equiv) was added to a solution of $\mathbf{1}\cdot(NTf_2)_8$, ^{19}F NMR (Figure S35) indicated that a large proportion of bound NTf_2^- was displaced by BF_4^-, as predicted from their binding constants (Table 1).

Having demonstrated the ability to follow anion displacement events with ^{19}F NMR, the different anion affinities of cages **1** and **2** allowed for the design of more complicated systems in which multiple guests' interactions with the two hosts could be studied. We first validated that cages **1** and **2**

dx.doi.org/10.1021/ja311882h | J. Am. Chem. Soc. 2013, 135, 5678−5684

Table 1. Summary of the Binding Constants of Anions for Cages 1 and 2

anion	binding affinity for cage **1** (M^{-1})	binding affinity for cage **2** (M^{-1})[b]
ClO_4^-[a]	$1.4(5) \times 10^4$	$5.7(2) \times 10^5$
BF_4^-[a,c]	$4.0(1) \times 10^3$	$2.3(4) \times 10^4$
OTf^-[a]	$3.0(1) \times 10^3$	$5.2(8) \times 10^4$
PF_6^-[a]	$2.8(1) \times 10^3$	$1.3(5) \times 10^6$
NTf_2^-	$1.4(5) \times 10^3$	no binding observed

[a]Binding affinities for these anions in cage **1** were obtained from competitive titration experiments (see Supporting Information). Standard deviations in the least significant digit are given in parentheses. [b]The value for ClO_4^- was determined as part of this study (Figure S32), whereas those for BF_4^-, OTf^-, and PF_6^- have been reported previously.[41] [c]A direct titration of excess BF_4^- into **1**·$(BF_4)_8$ yielded a similar value for the binding affinity of BF_4^- for cage **1** (Figure S21).

could be studied in solution together. No scrambling of aniline and anisidine residues was observed between the two cages during the titration experiments discussed below, and further experiments showed no evidence of scrambling by ^{1}H NMR and ESI-MS under the experimental conditions employed (Figures S39–S43). We infer that the imine exchange[52] observed in similar structures[41] is dependent on either the concentration of free aniline or water,[53] which have been minimized in the present experimental conditions.

The mechanism of anion encapsulation for cages **1** and **2** may take place via one of two possible processes, either by the diffusion of anions through the open faces of the cages assisted by twisting of the ligands, or by the dissociation of the ligands involving breakage of Fe–N bonds. Based upon investigations of similar systems,[32] we anticipate the rate of ligand dissociation for cages **1** and **2** to be in the range of 10^{-5}–10^{-6} s^{-1}.[32]

Only one set of cage signals was ever observed in NMR spectra of cage **1**, indicating that all guests investigated underwent fast exchange on the NMR time scale between the free and cage-bound states. Fast exchange of triflimide, the largest guest, was observed even at temperatures as low as 233 K (Figure S33). Similarly, NMR spectra of cage **2** in the presence of either BF_4^- or ClO_4^- displayed only one set of signals. The observation of fast exchange is consistent with an exchange rate of guests between the cage cavity and the bulk solution that is higher than the difference in frequency between fully bound host signal and free host signal in the NMR spectra. The difference between the ^{1}H NMR chemical shift values of the host's imine signal in the free and bound states was estimated to be ca. 40 Hz (0.1 ppm at 400 MHz, see Figures S19 and S32). This value would give an exchange rate $k_{ex} \approx 2.2\Delta\nu = 88$ s^{-1} at the coalescence temperature.[54] The rate of anion exchange at 298 K (a temperature much higher than the coalescence temperature, which must be below 233 K, as demonstrated by low temperature NMR experiments) is considerably greater than 88 s^{-1} and, therefore, more than 6 orders of magnitude faster than the most rapid ligand dissociation rate of 10^{-5}–10^{-6} s^{-1}.[32] We infer, thus, the guest exchange of these anions to take place through the faces of the host, on a significantly faster time scale than dynamic ligand exchange.

NMR spectra of cage **2** in the presence of PF_6^- and OTf^- showed slow guest exchange processes on the NMR time scale. To probe the guest exchange mechanism for these systems we determined the rates of guest exchange for OTf^-, the largest guest bound within **2**, by ^{1}H–^{1}H EXSY NMR experiments. At 298 K the first-order uptake rate constant k'_{in} of OTf^- into cage **2** was measured to be $(1.8 \pm 0.4) \times 10^{-2}$ s^{-1}, and the release rate constant was measured to be $(5.2 \pm 0.6) \times 10^{-2}$ s^{-1} (see Supporting Information). Both exchange rates are ca. three orders of magnitude higher than the rates of ligand dissociation,[32] leading us to conclude that the encapsulation mechanism for the "slowly" exchanging PF_6^- and OTf^- into cage **2** is also by diffusion of the guest through the faces of the cage.

Next, the interactions of a single anion within a 1:1 system of both cages **1** and **2** were studied in detail. Anion titration experiments were carried out with BF_4^-, PF_6^-, OTf^-, and ClO_4^- against an equimolar solution of both cages **1**·$(NTf_2)_8$ and **2**·$(NTf_2)_8$ in acetonitrile (Table 2 shows the results of anion titration experiments with 1 equiv of each anion). As expected, the first equivalent of each anion was encapsulated within empty cage **2**, and only after more than one equivalent had been introduced did the added anion begin to compete with triflimide to bind within cage **1**. We were able to combine the equilibrium expressions for anion binding within cages **1** and **2** with the binding constants tabulated in Table 1 to derive a series of analytical expressions for the composition of a system containing **1**, **2**, NTf_2^-, and each of the other anions.

The equilibrium that is set when mixing cage **1**·$(NTf_2)_8$ and cage **2**·$(NTf_2)_8$ with counteranionic guest G (where G = BF_4^-, OTf^-, PF_6^-, or ClO_4^-) starts with G encapsulated within cage **2**, because triflimide cannot enter cage **2**, then G will be transferred to cage **1**, leaving cage **2** empty:

$$G \subset \mathbf{2} + X \subset \mathbf{1} \rightleftharpoons \mathbf{2} + G \subset \mathbf{1} + X \quad (1)$$

The equilibrium constant for this equilibrium is given by eq 2:

$$K^* = \frac{[\mathbf{2}][G \subset \mathbf{1}][X]}{[G \subset \mathbf{2}][X \subset \mathbf{1}]} = \frac{[\mathbf{2}]}{[G \subset \mathbf{2}]}\frac{[G \subset \mathbf{1}]}{[X \subset \mathbf{1}]}[X] \quad (2)$$

where [**2**] is the concentration of empty cage **2**, [G⊂**1**] the concentration of cage **1** with anion G inside, [G⊂**2**] the

Table 2. Proportions of 1 equiv of Each Anionic Guest Encapsulated in Cages 1 and 2, and Free in Solution, As Determined from Titration Experiments Carried out on an Equimolar Solution of Cages 1·$(NTf_2)_8$ and 2·$(NTf_2)_8$

guest	y^a	$[\mathbf{1}]_0$ (M)	K^{1b}	K^{2c} (M^{-1})	q^d	$(1-y)-q^e$
ClO_4^-	0.93	5.0×10^{-4}	10.1(1)	$5.7(2) \times 10^5$	0.03	0.04
BF_4^-	0.87	1.0×10^{-3}	2.9(2)	$2.3(4) \times 10^4$	0.05	0.08
OTf^-	0.88	5.0×10^{-4}	2.2(1)	$5.2(8) \times 10^4$	0.04	0.08
PF_6^-	0.98	5.0×10^{-4}	2.1(4)	$1.3(5) \times 10^6$	0.01	0.01

[a]Fraction of cage **2** that incorporates guest. [b]Competitive binding constant of the guest against NTf_2^- for cage **1**. [c]Binding constant of the guest for empty cage **2**. For K^1 and K^2, standard deviations in the least significant digits are given in parentheses. [d]Fraction of cage **1** that incorporates guest. [e]Proportion of guest free in solution.

dx.doi.org/10.1021/ja311882h | J. Am. Chem. Soc. 2013, 135, 5678–5684

Scheme 2. Anion Exchange Sequence: Binding of ClO_4^- within Cage 2, Followed by Its Displacement by PF_6^-, and Subsequent Displacement of NTf_2^- from Cage 1 by the Released ClO_4^-

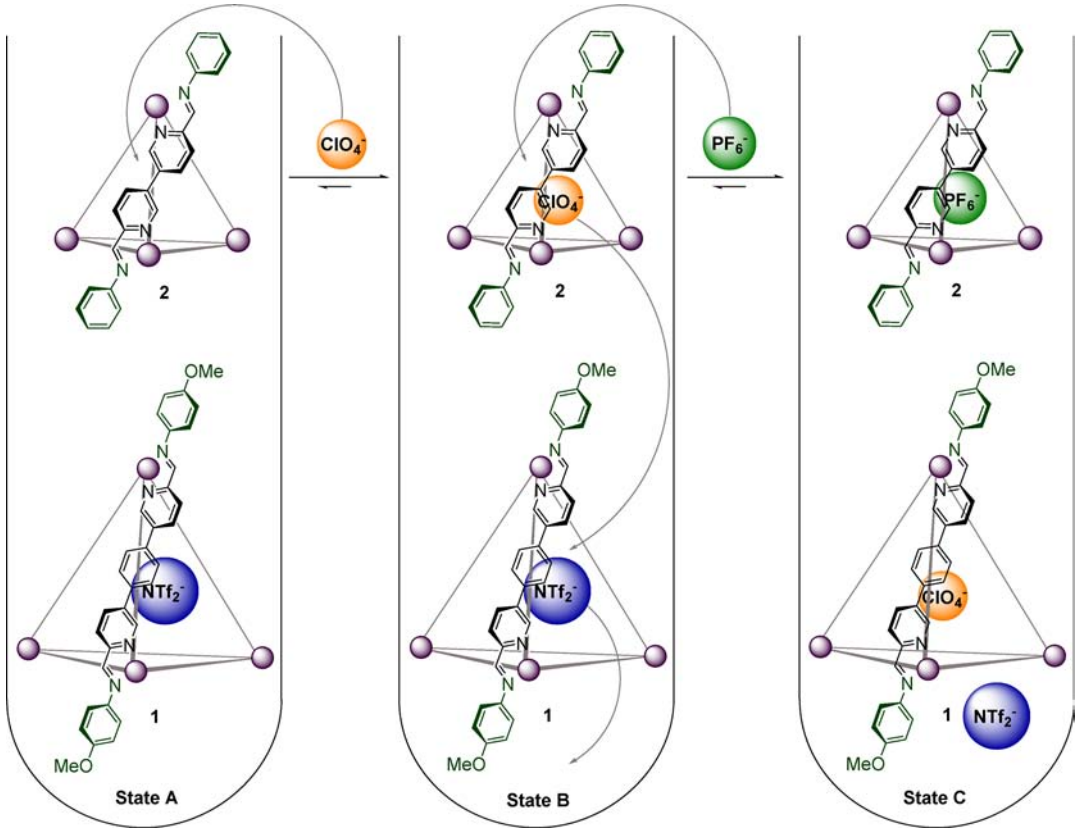

concentration of cage **2** with anion G inside, [X⊂**1**] the concentration of cage **1** with NTf_2^- inside, [X] the concentration of free NTf_2^-, K^1 the competitive binding constant of anion G against NTf_2^- for cage **1** and K^2 the binding constant of anion G to cage **2**.

With the assumption that cage **2** can only encapsulate anionic guest G (and not the NTf_2^- anion) and that no "empty" cage **1** is available, and by considering the mass balances for the total amount of host and guest species, the equilibrium of eq 1 can be rearranged into eq 3 (full derivations of all equations are reported in the Supporting Information):

$$K^* = \frac{K^1}{K^2} = \frac{[\mathbf{2}][\mathrm{G}\subset\mathbf{1}][\mathrm{X}]}{[\mathrm{G}\subset\mathbf{2}][\mathrm{X}\subset\mathbf{1}]} = \frac{q}{1-q}\frac{1-y}{y}[16-y][\mathbf{1}]_0 \quad (3)$$

where y is the fraction of cage **2** that incorporates guest G and q is the fraction of cage **1** that incorporates guest G. The $[X] = (16 - y)[1]_0$ term means that at the start of the experiment, of the 16 equiv of NTf_2^- per cage **1**, 15 equiv are free in solution and 1 equiv is incorporated in cage **1**. At equilibrium, as a result of displacement of the NTf_2^- anion by guest G in cage **1** the total number of equivalents of free NTf_2^- will have become 15 + (1 − y).

The degree of encapsulation of anions by cage **2** shown in Table 2 (term y) was calculated from the NMR titration experiments with a 1:1 system of cages **1** and **2**. For the fast-exchanging BF_4^- and ClO_4^-, we related the chemical shifts of the imine proton to the chemical shift of the same proton for an empty cage and for a cage completely bound with BF_4^- or ClO_4^-, and for the slow-exchanging OTf^- and PF_6^-, we used the comparison of the integration of the ^1H signal of the imine proton for both the empty and anion bound cages. The value q was determined by taking the previously determined binding constants, K^1 and K^2, the value of y as determined from ^1H NMR and the total concentration of cage **1**. Since the total concentration of the two hosts **1** and **2** and the guest G are all identical, the difference between (1 − y) and q represents the amount of guest G that is free in solution, as expressed in equivalents with respect to cage **1** (final column in Table 2).

From the comparison of the y and q values of all four anions, it can be seen that PF_6^- binds almost exclusively into cage **2**. It can also be observed that ClO_4^- competes most effectively with and thus is best at displacing NTf_2^- for cage **1**, and it is not the strongest binder for cage **2**, giving the possibility of it being displaced from **2** upon addition of PF_6^-. From this analysis a sequence which capitalizes upon this binding behavior can be deduced wherein an anion is displaced from cage **2** by the addition of another higher affinity anion, and the supplanted anion is then subsequently able to displace the anion already present in cage **1**, resulting in a chain-reaction exchange of different anions within the 1:1 two cage system (Scheme 2).

State **A** (Scheme 2) shows the initial equilibrium of the equimolar solution of cages **1**·$(NTf_2)_8$ and **2**·$(NTf_2)_8$, with cage **2** empty, and the 16 equiv of NTf_2^- present within the system saturating cage **1**. State **B** was thus entered into when 2 equiv of ClO_4^- were added to the system in state **A**, with the ClO_4^- anion saturating cage **2**, and a minority of the NTf_2^- being

dx.doi.org/10.1021/ja311882h | J. Am. Chem. Soc. 2013, 135, 5678−5684

displaced from cage **1** by the remaining ClO_4^-, as indicated by ^{19}F NMR (Figure S37). The addition of 1 equiv of PF_6^- then brought the system into state **C**, where PF_6^- had completely displaced the bound ClO_4^- from within cage **2** (Figure S36). The system's 2 equiv of ClO_4^- then acted to displace the majority of the NTf_2^- from cage **1** (Figure S37), resulting in a chain of anion exchange reactions.

For each of the states shown in Scheme 2, experiments and calculations thus reflect that the majority of each host binds the guest shown in each of the system's three states. The system's selectivity is imperfect, with cage **1**'s lack of differentiation between guests leaving room for future improvement. The large amount of NTf_2^- present within the starting system also reduces the system's selectivity; the use of a larger counterion, which does not bind to either **1** or **2**, proved infeasible due to the insolubility of the cages with larger anions. However, it is significant that displacement of a majority of the bound NTf_2^- could be achieved through the addition of only 2 equiv of ClO_4^-, despite the 16 equiv of NTf_2^- present in the system. The exchange sequence did not include OTf^- or BF_4^- due to the observation that their binding within cage **2** was not strong enough to displace bound perchlorate, and their binding with cage **1** was also too weak to displace a significant portion of NTf_2^-. Higher differentials between the affinities of **1** for different anions (Table 1) would be necessary to improve the selectivity of the system.

CONCLUSIONS

A cationic tetrahedral cage possessing a large enough cavity for the binding of the triflimide anion was synthesized via subcomponent self-assembly, and its host–guest chemistry with a selection of anions was studied. The interactions of the anions with an equimolar solution of this larger cage and a smaller cage were also studied in detail. The resultant anion-exchange sequence within the system of cages **1** and **2** demonstrates how different binding affinities may be harnessed in order to design sequential reactions in which guests are passed from one host to another. Although the selectivity in this chain-reaction is not optimal, it provides the foundation upon which future systems will be built. The coupling of improved chains to the functions of catalytic cages[14−19] could allow for the design of new chemical systems in which multiple reaction steps could be organized to progressively build up molecular complexity. Such linked networks of capsules could also serve to design indicator displacement assays[55,56] that respond differentially to combinations of analytes.

EXPERIMENTAL SECTION

All reagents and solvents were purchased from commercial sources and used as supplied. NMR spectra were recorded on a Bruker Avance DPX400 or DPX500 spectrometer; δ_H values are reported relative to acetonitrile-d_3 at 1.94 ppm. δ_C values are reported relative to acetonitrile-d_3 at 118.10 ppm. ^{19}F values are reported relative to the internal standard hexafluorobenzene at −166.70 ppm. Mass spectra provided by the EPSRC National MS Service Centre at Swansea were acquired on a Thermofisher LTQ Orbitrap XL. Low-resolution electrospray ionization mass spectra (ESI-MS) were obtained on a Micromass Quattro LC, infused from a Harvard Syringe Pump at a rate of 10 μL per minute. Cage **2** was synthesized as previously reported.[41] Iron(II) bis(trifluoromethane)sulfonamide dihydrate[41,57] and hexakis(acetonitrile)iron(II) hexafluorophosphate[32] were prepared as previously reported. The syntheses of 5,5′-(1,4-phenylene)-bis-2-pyridinecarboxaldehyde, **1**·$(BF_4)_8$, **1**·$(PF_6)_8$, and **1**·$(ClO_4)_8$ are reported in the Supporting Information.

Preparation of Cage 1·$(NTf_2)_8$. 5,5′-(1,4-Phenylene)bis-2-pyridinecarboxaldehyde (24 mg, 0.083 mmol), *p*-methoxyaniline (20 mg, 0.167 mmol), and iron(II) bis(trifluoromethane)sulfonimide dihydrate (34 mg, 0.055 mmol) were added to a 25 mL Schlenk flask containing degassed acetonitrile (6 mL). The flask was sealed and subjected to three evacuation/nitrogen fill cycles. The reaction was stirred for 24 h at 323 K. **1**·$(NTf_2)_8$ was precipitated as a green powder by the addition of diethyl ether (yield 48 mg, 66%). ^1H NMR (500 MHz, 298 K, CD_3CN): δ = 8.82 (s, 2H, imine), 8.66 (d, J = 8.5 Hz, 2H, pyridine), 8.57 (d, J = 8.0 Hz, 2H, pyridine), 7.47 (s, 4H, phenyl), 7.44 (s, 2H, pyridine), 6.79 (d, J = 8.5 Hz, 4H, *p*-methoxyaniline), 5.45 (s, DCM), 3.81 (s, 6H, methoxy); ^{13}C NMR (125 MHz, 298K, CD_3CN): δ = 173.90, 160.64, 158.33, 153.31, 144.17, 139.64, 137.56, 136.01, 131.04, 128.45, 123.78, 115.11, 56.22. ^{19}F NMR (376 MHz, 298 K, CD_3CN): δ = −81.41 (−81.33 for $LiNTf_2$). Elemental analysis (%) calcd for chemical formula: $C_{208}H_{156}F_{48}Fe_4N_{32}O_{44}S_{16}\cdot 11H_2O$: C, 44.18; H, 3.17; N, 7.93. Found: C, 44.13; H, 2.88; N, 7.84. *m/z*: 1538.5 $\{[\mathbf{1}\cdot(NTf_2)_5]^{3+}\}$, 1083.7 $\{[\mathbf{1}\cdot(NTf_2)_4]^{4+}\}$, 810.9 $\{[\mathbf{1}\cdot(NTf_2)_3]^{5+}\}$.

Crystallography. Data for **1**·$(BF_4)_8$ and **1**·$(ClO_4)_8$ were collected at Beamline I19 of Diamond Light Source employing silicon double crystal monochromated synchrotron radiation (0.6889 Å) with ω scans at 100(2) K.[58] Pictures of the crystal structure of $[(MeCN)_{1.5}(iPr_2O)0.5\subset\mathbf{1}]\cdot 8ClO_4\cdot 4MeCN\cdot iPr_2O$ and the crystal packing are shown in the Supporting Information (Figure S17). Data integration and reduction for $[(MeCN)_3\subset\mathbf{1}]\cdot 8BF_4\cdot 0.5MeCN$ were undertaken with CrystalClear[58] and data for $[(MeCN)_{1.5}(iPr_2O)$-$0.5\subset\mathbf{1}]\cdot 8ClO_4\cdot 4MeCN\cdot iPr_2O$ were first treated with ECLIPSE,[59] the cell orientations determined with CELL_NOW[60] and then integration and reduction performed with SAINT and XPREP.[61] Subsequent computations were carried out using the WinGX-32 graphical user interface.[62] Multiscan empirical absorption corrections were applied to the data using the programs CrystalClear[58] or TWINABS.[63] Structures were solved by charge flipping using SUPERFLIP[64] then refined and extended with SHELXH-97.[65] In general, non-hydrogen atoms with occupancies greater than 0.5 were refined anisotropically. Carbon-bound hydrogen atoms were included in idealized positions and refined using a riding model. The crystals were extremely unstable, rapidly decaying once removed from the mother liquor and required rapid handling at dry ice temperatures (<5 s) to facilitate data collection. The crystals were also weakly diffracting with very few reflections recorded at higher than 1.0 Å resolution for $[(MeCN)_3\subset\mathbf{1}]\cdot 8BF_4\cdot 0.5MeCN$ and 0.9 Å resolution for $[(MeCN)_{1.5}(iPr_2O)0.5\subset\mathbf{1}]\cdot 8ClO_4\cdot 4MeCN\cdot iPr_2O$. Accordingly there are a number of larger than ideal U_{eq} max/min ratios. Both structures show disorder in the solvent and anions and a number of constraints and restraints were required to facilitate realistic modeling. The crystallographic data are summarized below.

$[(MeCN)_3\subset\mathbf{1}]\cdot 8BF_4\cdot 0.5MeCN$. Formula $C_{199}H_{166.5}B_8F_{32}Fe_4N_{27.5}O_{12}$, M 4052.98, monoclinic, space group $P2_1/c$ (No. 14), a = 27.191(11), b = 39.825(15), and c = 20.852(8) Å, β = 96.369(3)°, V = 22442(15) Å^3, D_c 1.200 g cm^{-3}, Z = 4, crystal size 0.1 × 0.01 × 0.001 mm, dark green blade, temperature = 100(2) K, λ(synchrotron) = 0.68890 Å, μ(synchrotron) = 0.338 mm^{-1}, T(CrystalClear)$_{min,max}$ = 0.409, 1.000, $2\theta_{max}$ = 40.30, *hkl* range −27 27, −37 39, −20 20, N = 118110, N_{ind} = 23420 (R_{merge} = 0.1108), N_{obs} = 16737 ($I > 2\sigma(I)$), N_{var} = 2045, residuals $R1(F)$ = 0.1310, $wR2(F^2)$ = 0.3031, GoF(all) = 1.487, $\Delta\rho_{min,max}$ = −0.847, 1.318 e$^-$ Å^{-3}.

The positions of only four of the eight anions could be located with the remaining anions located in a region of smeared electron density. Despite numerous attempts at modeling this region of disorder as a combination of both disordered anions and solvent (including the use of rigid bodies) no successful model could be obtained and the data was treated with the SQUEEZE[66] function of PLATON,[67] which resulted in significantly better residuals.

$[(MeCN)_{1.5}(iPr_2O)_{0.5}\subset\mathbf{1}]\cdot 8ClO_4\cdot 4MeCN\cdot iPr_2O$. Formula $C_{212}H_{193.5}Cl_8Fe_4N_{29.5}O_{45.5}$, M 4389.46, triclinic, space group $P\bar{1}$ (No. 2), a = 20.495(9), b = 25.670(12), and c = 25.757(15) Å, α = 118.873(17), β = 109.64(4), and γ = 93.55(3)°, V = 10755(9) Å^3, D_c = 1.355 g cm^{-3}, Z = 2, crystal size 0.15 × 0.02 × 0.001 mm, dark green blade, temperature = 100(2) K, λ(synchrotron) = 0.68890 Å,

dx.doi.org/10.1021/ja311882h | J. Am. Chem. Soc. 2013, 135, 5678−5684

μ(synchrotron) = 0.446 mm^{-1}, T(TWINABS)$_{min,max}$ = 0.505585, 0.745532, $2\theta_{max}$ = 45.00, *hkl* range −22 21, −28 24, 0 28, N = 30953, N_{ind} = 30972 (R_{merge} = 0.1827), N_{obs} = 18574 ($I > 2\sigma(I)$), N_{var} = 2555, residuals $R1(F)$ = 0.0915, $wR2(F^2)$ = 0.2288, GoF(all) = 1.029, $\Delta\rho_{min,max}$ = −1.255, 1.692 e$^-$ Å^{-3}.

Despite appearing (at least visually) to be a single crystal, the sample employed in this study proved to be a twinned by a 2-fold rotation approximately around *c*. The BASF parameter refined to 0.55274. It was possible to locate the positions of all the ClO_4^- counterions (disordered over nine lattice sites) and the majority of the solvent molecules (with a remaining solvent accessible void of 100 Å^3 per unit cell) and SQUEEZE was not employed in this case. One of the central phenyl rings shows positional disorder and was modeled in two parts with isotropic thermal parameters. One of the periphery OMe groups shows some unresolved disorder and was also modeled isotropically. The occupancies of the two positions of the disordered solvent molecules inside the tetrahedral cavity were refined and then fixed at the obtained values.

K_a Determination. The derivation of the equations for competitive binding studies and of the expression of the fraction of occupied host as a function of total guest concentration was published elsewhere.[41] The binding isotherms for all competitive binding titration experiments show 1:1 binding for all anions. The concentration of cage **1**·$(NTf_2)_8$ was kept constant throughout all titration experiments and small aliquots of the second guest solution were titrated into a J-Young NMR tube containing **1**·$(NTf_2)_8$ before each spectrum was acquired. All NMR data and binding constant fittings are reported in the Supporting Information. The titration of fast exchanging [OTf$^-$] = 0.102 M guest into a solution of [**1**·$(NTf_2)_8$] = 3.4 × 10^{-3} M resulted in a relative binding constant of 2.21 ± 0.11. The titration of fast exchanging [PF_6^-] = 0.102 M guest into a solution of [**1**·$(NTf_2)_8$] = 3.4 × 10^{-3} M resulted in a relative binding constant of 2.06 ± 0.35. The titration of fast exchanging [BF_4^-] = 0.054 M guest into a solution of [**1**·$(NTf_2)_8$] = 1.8 × 10^{-3} M resulted in a relative binding constant of 2.93 ± 0.18. The titration of fast exchanging [ClO_4^-] = 0.022 M guest into a solution of [**1**·$(NTf_2)_8$] = 7.3 × 10^{-4} M resulted in a relative binding constant of 10.06 ± 1.12. Titration experiments with cage **1** formed with aniline and NMR titrations for the binding affinity of ClO_4^- for cage **2** are reported in the Supporting Information.

Estimates of the binding constants of triflimide for cage **1** were obtained by titrating excess NTf_2^- into solutions **1**·$(NTf_2)_8$. The derivation of the equations for these binding studies was published elsewhere.[41] The minimum of the total guest concentration (the X parameter) was set to 0 in the fitting model, and the initial chemical shift Y parameter was optimized by the binding algorithm to give a value of 7.40 ppm. The binding of NTf_2^- was therefore estimated to be (1.4 ± 0.5) × 10^3 M^{-1}. The concentration of cage **1**·$(NTf_2)_8$ was kept constant throughout the titration experiment and small aliquots of NTf_2^- solution were titrated into a J-Young NMR tube before each spectrum was acquired. [**1**·$(NTf_2)_8$] = 2.3 × 10^{-4} M. [NTf_2^-] = 0.003 M.

Estimates of the binding constants of BF_4^- for cage **1** were obtained by titrating excess BF_4^- into solutions **1**·$(BF_4)_8$. The concentration of cage **1**·$(BF_4)^8$ was kept constant throughout the titration experiment and small aliquots of BF_4^- solution were titrated into a J-Young NMR tube before each spectrum was acquired. [**1**·$(BF_4)_8$] = 2.3 × 10^{-4} M, [BF_4^-] = 0.003 M. The minimum of the total guest concentration (the X parameter) was set to 0 in the fitting model, and the initial parameter for Y was set to 7.40 ppm, and the binding of BF_4^- was estimated to be (4.9 ± 3.6) × 10^3 M^{-1}.

Anion Exchange Experiments. To investigate potential scrambling effects between the two cages, a 1:1 mixture of **1**·$(NTf_2)_8$ (1.0 mg, 2.1 × 10^{-7} mol, 1 equiv) and **2**·$(NTf_2)_8$ (1.1 mg, 2.1 × 10^{-7} mol, 1 equiv) dissolved in CD_3CN (0.5 mL) was sealed in a J-Young tube. The dark blue mixture was sonicated for 10 min before being subjected to ^{1}H NMR and ESI-MS analysis. Extra aniline (0.08 mg, 8.4 × 10^{-7} mol, 4 equiv) from a premade CD_3CN stock solution was added to the 1:1 cage mixture and left for 24 h at 323 K. ^{1}H NMR spectra and MS data of scrambling experiments are reported in the Supporting Information.

To study the rate of exchange for the largest guests into cages **1** and **2**, a solution of **1**·$(NTf_2)_8$ (2.0 mg, 3.6 × 10^{-7} mol, 8 equiv) in CD_3CN (0.5 mL) was sealed in a J-Young tube and the ^{1}H NMR spectrum was acquired at 233 K. To the same tube, tetrabutylammonium triflate (0.14 mg, 3.6 × 10^{-7} mol, 8 equiv) was added from a premade CD_3CN stock solution, and the solution was sealed in a J-Young tube and sonicated for 10 min. The ^{1}H NMR spectrum was again acquired at 233 K. 2D EXSY NMR experiments were run onto a solution of OTf$^-$⊂**2**·$(NTf_2)_8$ (7.0 mg, 3.8 × 10^{-3} mol, 1 equiv, OTf$^-$ 0.5 equiv) at 298 and 308 K. Rate constants are reported in the Supporting Information.

A 1:1 mixture of **1**·$(NTf_2)_8$ (1.0 mg, 1.8 × 10^{-7} mol, 1 equiv) and **2**·$(NTf_2)_8$ (1.1 mg, 2.1 × 10^{-7} mol, 1 equiv) dissolved in CD_3CN (0.4 mL) was sealed in a J-Young tube. The dark blue mixture was sonicated for 10 min. The concentration of the mixture of cages **1**·$(NTf_2)_8$ and **2**·$(NTf_2)_8$ was kept constant throughout the titration experiment and small aliquots of up to one equivalent of OTf$^-$, BF_4^-, PF_6^-, or ClO_4^- solution were titrated into the mixture before each spectrum was acquired. [cage] = 5.3 × 10^{-4} M. [anion] = 5.3 × 10^{-4} M. All NMR data are reported in the Supporting Information.

For anion exchange studies, a solution of **1**·$(NTf_2)_8$ (1.0 mg, 1.8 × 10^{-7} mol, 1 equiv) in CD_3CN (0.5 mL) was sealed in a J-Young tube and the dark green solution was sonicated for 10 min and the ^{19}F NMR spectrum was acquired. To the same tube, tetraethylammonium tetrafluoroborate (0.4 mg, 1.8 × 10^{-6} mol, 10 equiv) was added from a premade CD_3CN stock solution and the ^{19}F NMR spectrum was acquired after sonication for 20 min. A solution of **1**·$(NTf_2)_8$ (2.2 mg, 4.2 × 10^{-7} mol, 1 equiv) and **2**·$(NTf_2)_8$ (2.0 mg, 4.2 × 10^{-7} mol, 1 equiv) dissolved in CD_3CN (0.5 mL) were sealed in a J-Young tube. The dark blue mixture was sonicated for 10 min to give state **A**. To the same tube, tetrabutylammonium perchlorate (0.28 mg, 8.4 × 10^{-7} mol, 2 equiv) was added from a premade CD_3CN stock solution giving state **B**, and the ^{19}F NMR spectrum was acquired after sonication for 20 min. To the same tube tetrabutylammonium hexafluorophosphate (0.16 mg, 4.2 × 10^{-7} mol, 1 equiv) was added from a premade CD_3CN stock solution to give state **C**, and the ^{19}F NMR spectrum was again acquired after sonication for 20 min.

■ ASSOCIATED CONTENT

Ⓢ Supporting Information

Experimental procedures; ligand and cage characterization data; NMR titration studies; K_a determination; equilibrium equation derivation. This material is available free of charge via the Internet at http://pubs.acs.org. The crystallographic data have been deposited with the Cambridge Crystallographic Data Centre as entries CCDC 877966 and 877967.

■ AUTHOR INFORMATION

Corresponding Author

jrn34@cam.ac.uk

Present Addresses

[†]Biomolecular NanoTechnology Group, MESA+ Institute for Nanotechnology, University of Twente, PO Box 217, 7500AE Enschede, The Netherlands

[‡]School of Chemistry and Molecular Biosciences, The University of Queensland, Brisbane St Lucia, QLD, Australia 4072

Notes

The authors declare no competing financial interest.

■ ACKNOWLEDGMENTS

We thank the NMR service team at the Cambridge Chemistry Department for carrying out some of the NMR spectroscopy, the EPSRC Mass Spectrometry Service at Swansea for carrying out the high-resolution mass spectrometry, and the Diamond Light Source (UK) for synchrotron beamtime on I19 (MT6791

and MT7114). This research was funded by EPSRC. M.M.J.S. acknowledges The Netherlands Organization for Scientific Research (NWO Rubicon Fellowship), Y.R.H. acknowledges the Cambridge European Trust, and J.K.C. acknowledges the Marie Curie IIF scheme of the 7th EU Framework Program.

REFERENCES

(1) Furutani, Y.; Kandori, H.; Kawano, M.; Nakabayashi, K.; Yoshizawa, M.; Fujita, M. *J. Am. Chem. Soc.* **2009**, *131*, 4764.
(2) Gupta, S.; Choudhury, R.; Krois, D.; Brinker, U. H.; Ramamurthy, V. *J. Org. Chem.* **2012**, *77*, 5155.
(3) Mal, P.; Breiner, B.; Rissanen, K.; Nitschke, J. R. *Science* **2009**, *324*, 1697.
(4) Furusawa, T.; Kawano, M.; Fujita, M. *Angew. Chem., Int. Ed.* **2007**, *46*, 5717.
(5) Nakabayashi, K.; Ozaki, Y.; Kawano, M.; Fujita, M. *Angew. Chem., Int. Ed.* **2008**, *47*, 2046.
(6) Clever, G. H.; Tashiro, S.; Shionoya, M. *Angew. Chem., Int. Ed.* **2009**, *48*, 7010.
(7) Ariga, K.; Ito, H.; Hillab, J. P.; Tsukube, H. *Chem. Soc. Rev.* **2012**, *41*, 5800.
(8) Anslyn, E. V. *J. Org. Chem.* **2007**, *72*, 687.
(9) Rakow, N. A.; Suslick, K. S. *Nature* **2000**, *406*, 710.
(10) Buryak, A.; Severin, K. *J. Am. Chem. Soc.* **2005**, *127*, 3700.
(11) Carlier, P. R. *Angew. Chem., Int. Ed.* **2004**, *43*, 2602.
(12) Kirkorian, K.; Ellis, A.; Twyman, L. J. *Chem. Soc. Rev.* **2012**, *41*, 6138.
(13) Fabbrizzi, L. *Top. Curr. Chem.* **2012**, *323*, 127.
(14) Pluth, M. D.; Bergman, R. G.; Raymond, K. N. *Science* **2007**, *316*, 85.
(15) Yoshizawa, M.; Tamura, M.; Fujita, M. *Science* **2006**, *312*, 251.
(16) Murase, T.; Horiuchi, S.; Fujita, M. *J. Am. Chem. Soc.* **2010**, *132*, 2866.
(17) Yoshizawa, M.; Takeyama, Y.; Okano, T.; Fujita, M. *J. Am. Chem. Soc.* **2003**, *125*, 3243.
(18) Schmidtchen, F. P. *Angew. Chem., Int. Ed.* **1981**, *20*, 466.
(19) Leung, D. H.; Fiedler, D.; Bergman, R. G.; Raymond, K. N. *Angew. Chem., Int. Ed.* **2004**, *43*, 963.
(20) Koblenz, T. S.; Wassenaar, J.; Reek, J. N. H. *Chem. Soc. Rev.* **2008**, *37*, 247.
(21) Fischbach, M. A.; Walsh, C. T. *Chem. Rev.* **2006**, *106*, 3468.
(22) Cram, D. J.; Tanner, M. E.; Thomas, R. *Angew. Chem., Int. Ed.* **1991**, *30*, 1024.
(23) Horiuchi, S.; Murase, T.; Fujita, M. *J. Am. Chem. Soc.* **2011**, *133*, 12445.
(24) Yoshizawa, M.; Kusukawa, T.; Fujita, M.; Yamaguchi, K. *J. Am. Chem. Soc.* **2000**, *122*, 6311.
(25) Smulders, M. M. J.; Nitschke, J. R. *Chem. Sci.* **2012**, *3*, 785.
(26) Ma, D.; Hettiarachchi, G.; Nguyen, D.; Zhang, B.; Wittenberg, J. B.; Zavalij, P. Y.; Briken, V.; Isaacs, L. *Nat. Chem.* **2012**, *4*, 503.
(27) Custelcean, R.; Bonnesen, P. V.; Duncan, N. C.; Zhang, X. H.; Watson, L. A.; Van Berkel, G.; Parson, W. B.; Hay, B. P. *J. Am. Chem. Soc.* **2012**, *134*, 8525.
(28) Chakrabarty, R.; Mukherjee, P. S.; Stang, P. J. *Chem. Rev.* **2011**, *111*, 6810.
(29) Cangelosi, M. V.; Zakharov, L. N.; Fontenot, S. A.; Pitt, M. A.; Johnson, D. W. *Dalton Trans.* **2008**, 3447.
(30) Breiner, B.; Clegg, J. K.; Nitschke, J. R. *Chem. Sci.* **2011**, *2*, 51.
(31) Liu, Y. Z.; Hu, C. H.; Comotti, A.; Ward, M. D. *Science* **2011**, *333*, 436.
(32) Clegg, J. K.; Cremers, J.; Hogben, A. J.; Breiner, B.; Smulders, M. M. J.; Thoburn, J. D.; Nitschke, J. R. *Chem. Sci.* **2013**, *4*, 68.
(33) Qiu, W.; Perman, J. A.; Wojtas, L.; Eddaoudi, M.; Zaworotko, M. J. *Chem. Commun.* **2010**, *46*, 8734.
(34) Olive, A. G. L.; Parkan, K.; Givelet, C.; Michl, J. *J. Am. Chem. Soc.* **2011**, *133*, 20108.
(35) Zebret, S.; Dupont, N.; Bernardinelli, G.; Hamacek, J. *Chem.—Eur. J.* **2009**, *15*, 3355 .
(36) Cangelosi, V. M.; Zakharov, L. N.; Johnson, D. W. *Angew. Chem., Int. Ed.* **2010**, *49*, 1248.
(37) Turega, S.; Whitehead, M.; Hall, B. R.; Haddow, M. F.; Hunter, C. A.; Ward, M. D. *Chem. Commun.* **2012**, *48*, 2752.
(38) Albrecht, M.; Shang, Y. L.; Rhyssen, T.; Stubenrauch, J.; Winkler, H. D. F.; Schalley, C. A. *Eur. J. Org. Chem.* **2012**, 2422.
(39) Ronson, T. K.; Fisher, J.; Harding, L. P.; Rizkallah, P. J.; Warren, J. E.; Hardie, M. J. *Nat. Chem.* **2009**, *1*, 212.
(40) Ousaka, N.; Grunder, S.; Castilla, A. M.; Whalley, A. C.; Stoddart, J. F.; Nitschke, J. R. *J. Am. Chem. Soc.* **2012**, *134*, 15528.
(41) Hristova, Y. R.; Smulders, M. M. J.; Clegg, J. K.; Breiner, B.; Nitschke, J. R. *Chem. Sci.* **2011**, *2*, 638.
(42) Campbell, V. E.; Nitschke, J. R. *Synlett* **2008**, *20*, 2077.
(43) Domer, J.; Slootweg, J. C.; Hupka, F.; Lammertsma, K.; Hahn, F. E. *Angew. Chem., Int. Ed.* **2010**, *49*, 6430.
(44) Zhou, X.-P.; Liu, J.; Zhan, S.-Z.; Yang, J.-R.; Li, D.; Ng, K.-M.; Sun, R. W.-Y.; Che, C.-M. *J. Am. Chem. Soc.* **2012**, *134*, 8042.
(45) Nowell, H.; Barnett, S. A.; Christensen, K. E.; Teat, S. J.; Allan, D. R. *J. Synchrotron Radiat.* **2012**, *19*, 435.
(46) Meng, W.; Clegg, J. K.; Thoburn, J. D.; Nitschke, J. R. *J. Am. Chem. Soc.* **2011**, *133*, 13652.
(47) Scherer, M.; Caulder, D. L.; Johnson, D. W.; Raymond, K. N. *Angew. Chem., Int. Ed.* **1999**, *38*, 1588.
(48) Biros, S. M.; Yeh, R. M.; Raymond, K. N. *Angew. Chem., Int. Ed.* **2008**, *47*, 6062.
(49) Sessler, J. L.; Camiolo, S.; Gale, P. A. *Coord. Chem. Rev.* **2003**, *240*, 17.
(50) Hua, Y. R.; Flood, A. H. *Chem. Soc. Rev.* **2010**, *39*, 1262.
(51) Chung, M. K.; Severin, K.; Lee, S. J.; Waters, M. L.; Gagne, M. R. *Chem. Sci.* **2011**, *2*, 744.
(52) Belowich, M. E.; Stoddart, J. F. *Chem. Soc. Rev.* **2012**, *41*, 2003.
(53) Dirksen, A.; Dirksen, S.; Hackeng, T. M.; Dawson, P. E. *J. Am. Chem. Soc.* **2006**, *128*, 15602.
(54) Sanders, J. K. M.; Hunter, B. K. *Modern NMR Spectroscopy: A Guide for Chemists*; Oxford University Press: Oxford, UK, 1993.
(55) Nguyen, B. T.; Anslyn, E. V. *Coord. Chem. Rev.* **2006**, *250*, 3118.
(56) Severin, K. *Chem. Commun.* **2006**, *42*, 3859.
(57) Sibi, M. P.; Petrovic, G. *Tetrahedron: Asymmetry* **2003**, *14*, 2879.
(58) Rigaku *CrystalClear*; Rigaku Americas and Rigaku Corporation: Texas, 1997−2009.
(59) Parsons, S. *ECLIPSE*; The University of Edinburgh: Edinburgh, UK, 2004.
(60) Bruker-Nonius *Cell_NOW*; Bruker AXS Inc.: Madison, WI, 2003.
(61) Bruker-Nonius *APEX* v2.1, *SAINT* v.7, and *XPREP* v.6.14; Bruker AXS Inc.: Madison, WI, 2003.
(62) Farrugia, L. J. *J. Appl. Crystallogr.* **1999**, *32*, 837.
(63) Sheldrick, G. *SADABS: Empirical Absorption and Correction Software*: University of Göttingen: Germany, 1996−2008.
(64) Palatinus, L.; Chapuis, G. *J. Appl. Crystallogr.* **2007**, *40*, 786.
(65) Sheldrick, G. M. *SHELX-97: Programs for Crystal Structure Analysis*; University of Göttingen: Göttingen, 1997.
(66) van der Sluis, P.; Spek, A. L. *Acta Crystallogr., Sect. A: Found. Crystallogr.* **1990**, *46*, 194.
(67) Spek, A. L. *PLATON: A Multipurpose Crystallographic Tool*; Utrecht University: Utrecht, The Netherlands, 2008.